

Determination of adsorption geometry on spherical particles from nonlinear Mie theory analysis of surface second harmonic generation

Grazia Gonella* and Hai-Lung Dai

Department of Chemistry, Temple University, Philadelphia, Pennsylvania 19122, USA

(Received 25 July 2011; published 8 September 2011)

Although second harmonic generation is intrinsically sensitive for probing interfaces, interpreting experimental observations for the determination of interfacial properties of colloidal particles requires rigorous theoretical treatment. A generally applicable nonlinear Mie theory is expanded into higher multipolar terms for describing second harmonic scattering from the surface of spherical particles. From a nonlinear least-square fitting of the scattering angular distribution of second harmonic light from molecules adsorbed on the surface, we demonstrate the determination of molecular hyperpolarizability and adsorption geometry on the surface of nanometer- to micrometer-sized spherical particles.

DOI: [10.1103/PhysRevB.84.121402](https://doi.org/10.1103/PhysRevB.84.121402)

PACS number(s): 42.25.Fx, 42.65.Ky, 82.70.Dd, 68.43.—h

Nonlinear light scattering (NLS), in the form of second harmonic and sum-frequency generation (SHG and SFG), has been used in recent years to study the surface of a variety of systems extending from flat surfaces in vacuum and gas to colloidal systems such as droplets,^{1–4} vesicles,^{5–8} and nanoparticles.^{9–37} The unique surface sensitivity of SHG and SFG makes these optical techniques optimal tools for the chemical and structural characterization of interfaces buried deep in the colloidal medium. A significant challenge in understanding NLS from the surface of a colloidal object is the description of the relation between the fundamental light(s) and the scattered nonlinear light as well as the influence of the particle and surface structures on the nonlinear optical process. For example, the scattering angular distribution of the SH light generated by molecules adsorbed on the surface of spherical particles depends not only on the directionality of the molecular hyperpolarizability and the adsorption geometry, but also on the size and refractive index of the particle.^{19,38–41} How to correctly interpret the experimentally observed SHG and relate it to the molecular properties and adsorption configuration requires a rigorous theoretical description of NLS from particles of any size and material.

At present, three main theoretical frameworks are available to describe NLS: the nonlinear Rayleigh-Gans-Debye theory (NLRGD),^{18,19,33,38,42,43} the nonlinear Wentzel-Kramers-Brillouin theory (NLWKB),¹⁹ and the nonlinear Mie theory (NLM).^{40,41,44–46} While the first two methods are easier to implement analytically, as they do not require obtaining the exact solution to the Maxwell equations, they are more restrictive in applications due to limitations associated with the assumptions that these models employ: The refractive index mismatch between the particle and the external medium as well as the particle size have to be small. In a previous work³² we have used the NLRGD theory to describe the scattering angular distribution and the effect of the particle size on the intensity of SHG from the model system consisting of malachite green molecules (MG) adsorbed on spherical plain polystyrene particles (PPS) (Fig. 1) in acidic aqueous solutions.⁴⁷ In this system the difference in refractive index between the particle and water is small (1.6 vs 1.34), nonetheless, it was shown that the NLRGD model cannot adequately describe the second harmonic scattering (SHS) patterns for particles whose diameter is in the micrometer size range.

In the development of the Mie theory for describing the NLS from the surface of spherical particles, there have been several recent advancements. Dadap *et al.* devised a NLM theory up to second order in the multipole expansion of the SH electromagnetic (e.m.) field suitable only for nanometer-sized particles.⁴⁶ Pavlyukh and Hübner reported the NLM model developed for particles of any size but applicable only when the effective charge is isotropic,⁴⁰ as pointed out by de Beer and Roke.⁴¹ The latter combined the NLM theory with the principle of time reversal to describe both SH and SF scattering, though this treatment is less effective in describing the near-field detection. In this Rapid Communication we present a further development of the NLM model as first laid out by Dadap *et al.*⁴⁶ to include higher-order multipoles in order to make it suitable for describing SHS from spherical particles of any size.

As a demonstration of the utility of the NLM model we have developed in this Rapid Communication, which uses general boundary conditions and a higher-order multipole expansion, we analyze the angular scattering distribution of the SH signal from the MG/PPS system for the determination of the adsorption geometry of MG on the particle surface.

In our experiments, which have been reported previously,^{29,32} the SH signal from PPS prior to MG adsorption was negligible in comparison to that detected after MG adsorption. The SH intensity measured as a function of the scattering angle in the horizontal plane for two different polarization combinations and several particle diameters ($d = 56, 88, 202, \text{ and } 1053 \text{ nm}$) is shown in Fig. 2.

NLM can be considered as the extension of the Mie theory that was originally derived for linear light scattering. Briefly, the incoming fundamental light (a plane wave) is projected onto the vector spherical harmonics basis set $\{Y_{l,m}(\theta, \phi)\hat{r}, X_{lm}(\theta, \phi), \hat{r} \times X_{lm}(\theta, \phi)\}$.^{48,49} The driving fundamental field at the particle surface $E'(\omega)$ is determined by applying the boundary conditions. Subsequently, the surface nonlinear polarizability can be expressed as $P_S(2\omega) = \chi^S : E'(\omega)E'(\omega)\delta(r - a)$, where χ^S is the macroscopic susceptibility of the surface, in the present case arising from the MG layer, while δ indicates the Dirac delta function. The nonvanishing tensor elements, assuming an isotropic symmetry in the surface plane, are $\chi_{\perp\perp\perp}^S, \chi_{\perp\parallel\parallel}^S, \chi_{\parallel\perp\parallel}^S = \chi_{\parallel\parallel\perp}^S$ (where \perp and \parallel refer to perpendicular and parallel to the

surface, respectively; see Fig. 1). After expressing the SH e.m. field generated on the vector spherical harmonics basis set, and after applying the appropriate boundary conditions,⁴⁶ with a

surface charge density $\sigma = -\nabla \cdot \mathbf{P}_S(2\omega)$ and surface current $\mathbf{j} = d\mathbf{P}_S(2\omega)/dt$, it is possible to express the SH field in the far region as

$$\mathbf{E}^{\text{sc}}(2\omega) = -E_0^2 \frac{e^{iK_1 r}}{K_1 r} \sum_{l=1}^{\infty} \sum_{m_{\text{even}}=-l}^l (-i)^l [iA_M^{2\omega, \text{sc}}(l, m) \mathbf{X}_{lm} - A_E^{2\omega, \text{sc}}(l, m) \hat{\mathbf{r}} \times \mathbf{X}_{lm}], \quad (1a)$$

$$\mathbf{B}^{\text{sc}}(2\omega) = -E_0^2 \frac{e^{iK_1 r}}{K_1 r} \sum_{l=1}^{\infty} \sum_{m_{\text{even}}=-l}^l (-i)^l \sqrt{\varepsilon_1(2\omega)} [A_E^{2\omega, \text{sc}}(l, m) \mathbf{X}_{lm} + iA_M^{2\omega, \text{sc}}(l, m) \hat{\mathbf{r}} \times \mathbf{X}_{lm}]. \quad (1b)$$

The expansion coefficients $A_M^{2\omega, \text{sc}}$ and $A_E^{2\omega, \text{sc}}$ derived from our calculations are

$$A_M^{2\omega, \text{sc}}(l, m) = \frac{4\pi K^2 r \chi_{\parallel\perp\parallel} b_{\perp\perp\parallel, M}^{lm} j(K_2 r)}{h(K_1 r) \frac{d}{dr} [rj(K_2 r)] - j(K_2 r) \frac{d}{dr} [rh(K_1 r)]} \Big|_{r=a}, \quad (2a)$$

$$A_E^{2\omega, \text{sc}}(l, m) = 4\pi K_1 \frac{i \frac{\varepsilon_2(2\omega)}{\varepsilon'(2\omega)} \sqrt{l(l+1)} (\chi_{\perp\perp\perp} b_{\perp\perp\perp}^{lm} + \chi_{\perp\parallel\parallel} b_{\perp\parallel\parallel}^{lm}) j(K_2 r) - \chi_{\parallel\perp\perp} b_{\parallel\perp\perp, E}^{lm} \frac{d}{dr} [rj(K_2 r)]}{\varepsilon_2(2\omega) j(K_2 r) \frac{d}{dr} [rh(K_1 r)] - \varepsilon_1(2\omega) h(K_1 r) \frac{d}{dr} [rj(K_2 r)]} \Big|_{r=a}. \quad (2b)$$

E_0 represents the amplitude of the incident fundamental field, a the particle radius, and $\varepsilon_1(\Omega)$, $\varepsilon'(\Omega)$, and $\varepsilon_2(\Omega)$ the dielectric functions of the external, superficial, and internal particle medium, respectively. The SH wave vectors $K = 2\pi/\lambda_{2\omega} = 2\omega/c$ in vacuum and $K_i = \sqrt{\varepsilon_i(2\omega)}K$, $i = 1, 2$ outside and inside the particle, respectively. $j(K_2 r)$ and $h(K_1 r)$ are the spherical Bessel function inside the particle and the spherical Hankel function of the first kind outside the particle, respectively. The b^{lm} coefficients represent the coefficients of the expansion of $\mathbf{P}_S(2\omega)$ on the vector spherical harmonics basis set $\mathbf{P}_S(2\omega) = \sum_{l, m} (\chi_{\perp\perp\perp} b_{\perp\perp\perp}^{lm} + \chi_{\perp\parallel\parallel} b_{\perp\parallel\parallel}^{lm}) Y_{lm} \hat{\mathbf{r}} + \chi_{\parallel\perp\parallel} (b_{\perp\perp\parallel, M}^{lm} \mathbf{X}_{lm} + b_{\perp\perp\parallel, E}^{lm} \hat{\mathbf{r}} \times \mathbf{X}_{lm})$. For further details on the NLM theory, the reader is referred to the Supplemental Material.⁴⁷ In this study we have used $\varepsilon_1(\omega) = (1.33)^2$ and $\varepsilon_1(2\omega) = (1.34)^2$ for H₂O,⁵⁰ $\varepsilon_2(\omega) = (1.58)^2$ and $\varepsilon_2(2\omega) = (1.62)^2$ for PS,⁵¹ and $\varepsilon'(\omega) = (1.54)^2$ and $\varepsilon'(2\omega) = (1.46 + i0.15)^2$ for the interface. The interface dielectric values have been obtained by first using the Bruggeman effective-medium approximation⁵² for the PS/H₂O interface with 50% PS and 50% H₂O volume fractions, followed by the Maxwell-Garnett effective-medium approximation⁵² assuming a 90% of the volume occupied by the PS/H₂O mixture and a 10% by MG,^{53,54} as previously evaluated by adsorption measurements.^{21,24} The

highest multipole considered (l_{max}), based on a particle size of 1053 nm, is 20.

MG is a planar molecule (in the molecular $x''z''$ plane) with C_{2v} symmetry (z'' as the C_2 rotation axis) as shown in Fig. 1. In general, a planar C_{2v} -symmetric molecule has three unique nonvanishing elements in the hyperpolarizability tensor β : In the molecular frame they are $\beta_{z''z''z''}$, $\beta_{z''x''x''}$, and $\beta_{x''x''x''} = \beta_{x''z''z''}$. Kikteva *et al.* have found that in the wavelength range considered in this study, β is dominated by $\beta_{z''x''x''}$ and $\beta_{x''z''z''}$.⁵⁵ In general, the macroscopic susceptibility elements expressed in the surface local coordinates can be related to the molecular β tensor elements through the Euler angles, Θ (tilt), Φ (azimuth), and Ψ (twist), as shown in Fig. 1, as $\chi_{ijk}^S = N_S \sum_{\text{abc}} \langle R_{ia} R_{jb} R_{kc} \rangle \beta_{\text{abc}}$, where the brackets indicate the ensemble orientational average. For an ensemble of molecules with surface density N_S , which are assumed to be distributed isotropically over the angles Φ and Ψ , the χ^S elements are

$$\chi_{\perp\perp\perp}^S = N_S/2 \langle \cos \Theta \sin^2 \Theta \rangle (\beta_{z''x''x''} + 2\beta_{x''z''z''}), \quad (3a)$$

$$\chi_{\perp\parallel\parallel}^S = N_S/2 \left[-\frac{1}{2} \langle \cos \Theta \sin^2 \Theta \rangle (\beta_{z''x''x''} + 2\beta_{x''z''z''}) + \langle \cos \Theta \rangle \beta_{z''x''x''} \right], \quad (3b)$$

$$\chi_{\parallel\perp\parallel}^S = N_S/2 \left[-\frac{1}{2} \langle \cos \Theta \sin^2 \Theta \rangle (\beta_{z''x''x''} + 2\beta_{x''z''z''}) + \langle \cos \Theta \rangle \beta_{x''z''z''} \right]. \quad (3c)$$

Equation (3) depends only on the β nonvanishing element ratio and on the angular distribution of the molecular tilt angle Θ , which may be determined from the ratios of the surface susceptibility tensor elements.⁵⁶⁻⁵⁸ From Eq. (3) we obtain the order parameter D , which relates to the distribution of Θ , and the ratio between the nonvanishing β tensor elements as

$$D(\Theta_0, \sigma) \equiv \frac{\langle \cos^3 \Theta \rangle}{\langle \cos \Theta \rangle} = \frac{\chi_{\perp\perp\perp}^S + 2\chi_{\perp\parallel\parallel}^S + 4\chi_{\parallel\perp\parallel}^S}{3\chi_{\perp\perp\perp}^S + 2\chi_{\perp\parallel\parallel}^S + 4\chi_{\parallel\perp\parallel}^S}, \quad (4a)$$

$$\frac{\beta_{x''z''z''}}{\beta_{z''x''x''}} = \frac{\chi_{\perp\perp\perp}^S + 2\chi_{\perp\parallel\parallel}^S}{\chi_{\perp\perp\perp}^S + 2\chi_{\perp\parallel\parallel}^S}, \quad (4b)$$

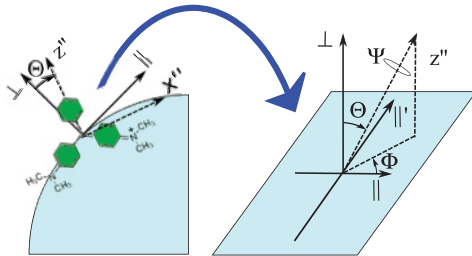


FIG. 1. (Color online) MG structure and relation between the surface local coordinate system ($\parallel, \parallel', \perp$) and the molecular reference frame (x'', y'', z'') (blown up on the right-hand side). Given the isotropicity of the surface $\parallel \equiv \parallel'$. Drawing not to scale.

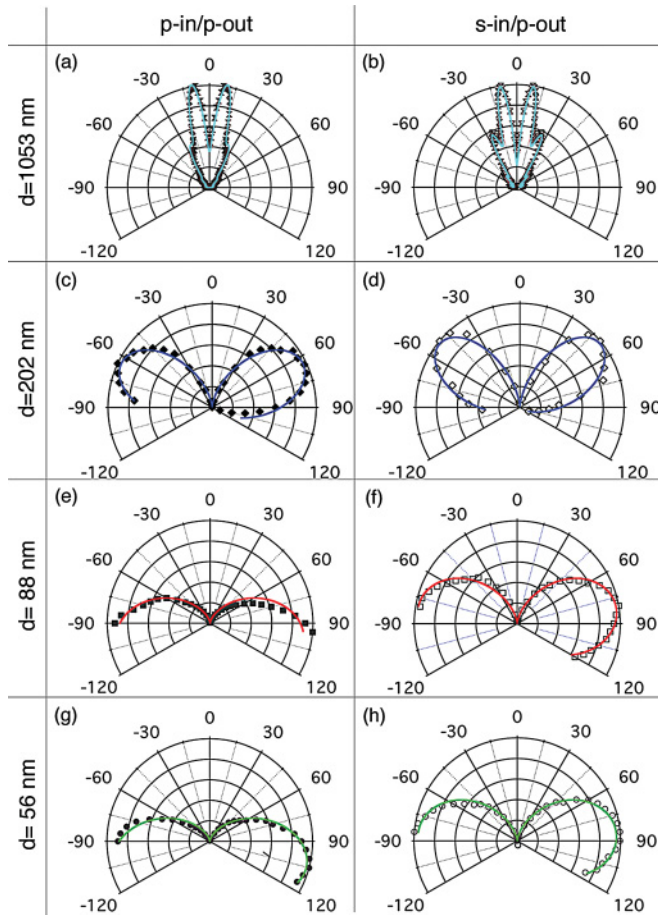


FIG. 2. (Color online) The best NLM model fit to the experimental data (SH intensity vs scattering angle Θ) for different particle diameters and polarization combinations. $\Theta = 0$ indicates the fundamental propagation direction. The fundamental wavelength is 840 nm.

where Θ_0 and σ are the tilt angle distribution's center and width, respectively. Eqs. (1) and (2) allow the calculation of the angular scattering pattern of the SH intensity generated from the surface of a spherical particle of a specific size and dielectric function. Since the molecular density, $\sim 4 \times 10^{13}$ molecules/cm², does not change appreciably with the particle size^{21,24} and the particle sizes considered are big enough compared to the MG molecule to disregard any surface curvature effects, we have further assumed that the adsorption configuration of MG molecules does not change with the particle size. From simultaneous nonlinear least-squares fitting of all of our data (shown in Fig. 2) we obtain $\chi_{\perp\perp\perp}^S/\chi_{\perp\parallel\parallel}^S = 0.43 \pm 0.02$ and $\chi_{\parallel\perp\parallel}^S/\chi_{\perp\parallel\parallel}^S = -0.23 \pm 0.01$, and, consequently, $D(\Theta_0, \sigma) = 0.64 \pm 0.01$ and $\beta_{x''z''x''}/\beta_{z''x''x''} = -0.01 \pm 0.01$. The fact that $\beta_{z''x''x''}$ is the dominant element can be found self-consistently by assuming in the very beginning that $\beta_{x''z''x''} = 0$.⁴⁷ It is not trivial to determine the molecular orientation from the relative ratios of the χ^S elements. We assume that the Θ distribution is represented by a normalized truncated Gaussian centered at Θ_0 and with standard deviation σ .^{58,59} Once the value of D is known, from Eq. (4) it is possible to find the pairs (Θ_0, σ) solution to the equation by intersecting the surface

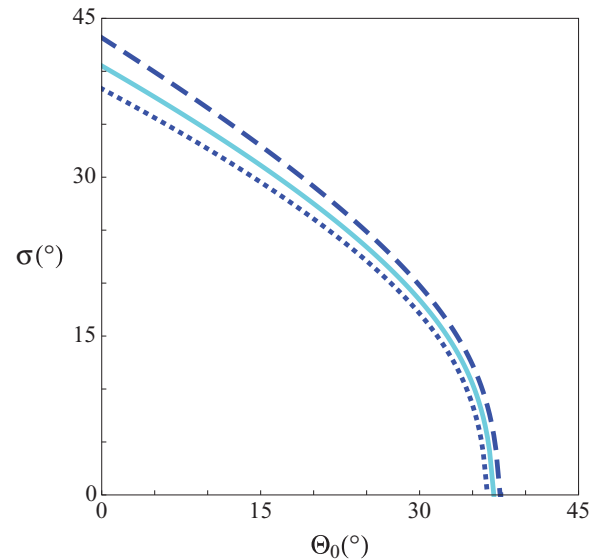


FIG. 3. (Color online) Locus of the pairs (Θ_0, σ) satisfying $D = 0.64$ (continuous line), as well as 0.63 (dashed line) and 0.65 (dotted line).

$\langle \cos^3 \Theta \rangle / \langle \cos \Theta \rangle$ with the plane D (for details, see Ref. 59). Figure 3 shows there is indeed some order⁵⁸ in the tilt angle of MG adsorbed on the PPS surface. The locus of the pair of parameters reported in Fig. 3, although does not allow for the determination of a single solution defining (Θ_0, σ) , indicates that the MG molecules stand quite upright, with a Θ assuming any values in between $(0 \pm 41)^\circ$ and $(37 \pm 0)^\circ$. Since SHG is sensitive to the angle of the polarization with respect to the surface normal, but not to its direction, the solutions in Fig. 3 show just one possible configuration for MG adsorption, the other being symmetric with respect to the axis $\Theta_0 = 90^\circ$: The MG dimethylamino groups either point away from the surface or toward it. The ζ -potential for the 1- μ m PS particle at pH \sim 4.1 has been measured to be -53 ± 6 mV.⁴⁷ The negative value for the PS surface charge and the positive charge for the MG dimethylamino group suggest the latter configuration, as shown in Fig. 1, to be more favorable.

In a previous work,³² using the NLRGD theory to analyze the same set of data, $\chi_{\perp\parallel\parallel}^S$ was found to be the dominant χ^S element, consistent with what we have obtained in this work. The exact χ^S element ratios, however, could not be determined. Furthermore, for the 1- μ m particle, the NLRGD model was not able to simulate the scattering angle patterns since this size is outside its range of applicability. With the NLM model the exact ratios $\chi_{\perp\perp\perp}^S/\chi_{\perp\parallel\parallel}^S$ and $\chi_{\parallel\perp\parallel}^S/\chi_{\perp\parallel\parallel}^S$ cannot be accurately determined using only the three smaller particles' data.⁴³ As the data of the micrometer-sized particle are added in, the multiplicity in the number of solutions is removed and the best NLM fit, shown in Fig. 2, leads to the values reported above and enables the determination of the MG tilt angle distribution.

A very recent study by Schürer *et al.* has used the NLM theory to analyze the SH scattering from 200-nm-diam PS particles without molecular adsorption and determined $\chi_{\perp\perp\perp}^S$ as the dominating χ^S element.⁶⁰ Earlier, Yang *et al.* examined the SH scattering pattern from MG adsorbed on polystyrene particles ($d = 510$ – 980 nm) terminated with carboxyl groups.¹⁵

Their NLRGD model analysis assumed a single $\chi_{\perp\perp\perp}^S$ element for the surface susceptibility tensor. Both cases dealt with systems different from ours. On the other hand, we note that our findings on the dominating molecular hyperpolarizability and the MG adsorption geometry agree well with a study of MG on silica, a flat surface with similar charge characteristics.⁵⁵

In summary, we have laid out the framework for calculating the scattering of the SH intensity generated from a monolayer of molecules adsorbed on a spherical particle using the NLM theory with the proper boundary conditions. We have shown that the NLM theory can be used to fit the experimental scattering pattern of SHG from any particle size, and that

such an analysis enables the determination of the adsorption configuration and the hyperpolarizability of the molecules adsorbed on the particle surface. The NLM theory extends the predictive power beyond that of the NLRGD model, which is limited by the refractive index matching and the particle size.

This work is supported in part by a grant from the Air Force Office for Scientific Research (FA9550-08-1-0092). The authors wish to thank J. Drazenovic and S. Savarala for the ζ -potential measurements, M. Ilies for the use of the Malvern ZS Nano instrument, and J. Dadap, A. de Beer, S. Roke, W. Gan, J. Smith, and S. L. Wunder for useful discussions.

*gonella@temple.edu

¹J. M. Hartings, A. Poon, X. Pu, R. K. Chang, and T. M. Leslie, *Chem. Phys. Lett.* **281**, 389 (1997).

²H. B. de Aguiar, A. G. F. de Beer, M. L. Strader, and S. Roke, *J. Am. Chem. Soc.* **132**, 2122 (2010).

³H. B. de Aguiar, M. L. Strader, A. G. F. de Beer, and S. Roke, *J. Phys. Chem. B* **115**, 2970 (2011).

⁴R. Vacha, S. W. Rick, P. Jungwirth, A. G. F. de Beer, H. B. de Aguiar, J.-S. Samson, and S. Roke, *J. Am. Chem. Soc.* **133**, 10204 (2011).

⁵A. Srivastava and K. B. Eisenthal, *Chem. Phys. Lett.* **292**, 345 (1998).

⁶E. C. Y. Yan and K. B. Eisenthal, *Biophys. J.* **79**, 898 (2000).

⁷V. Boutou, C. Favre, L. Woeste, and J.-P. Wolf, *Opt. Lett.* **30**, 759 (2005).

⁸J. Liu, M. Subir, K. Nguyen, and K. B. Eisenthal, *J. Phys. Chem. B* **112**, 15263 (2008).

⁹H. Wang, E. C. Y. Yan, E. Borguet, and K. B. Eisenthal, *Chem. Phys. Lett.* **259**, 15 (1996).

¹⁰F. W. Vance, B. I. Lemon, and J. T. Hupp, *J. Phys. Chem. B* **102**, 10091 (1998).

¹¹E. C. Y. Yan and K. B. Eisenthal, *J. Phys. Chem. B* **103**, 6056 (1999).

¹²Y. Liu, J. I. Dadap, D. Zimdars, and K. B. Eisenthal, *J. Phys. Chem. B* **103**, 2480 (1999).

¹³H. F. Wang, T. Troxler, A. G. Yeh, and H. L. Dai, *Langmuir* **16**, 2475 (2000).

¹⁴H. A. Clark, P. J. Campagnola, J. P. Wuskell, A. Lewis, and L. M. Loew, *J. Am. Chem. Soc.* **122**, 10234 (2000).

¹⁵N. Yang, W. E. Angerer, and A. G. Yodh, *Phys. Rev. Lett.* **87**, 103902 (2001).

¹⁶E. C. Hao, G. C. Schatz, R. C. Johnson, and J. T. Hupp, *J. Chem. Phys.* **117**, 5963 (2002).

¹⁷W. L. Mochan, J. A. Maytorena, B. S. Mendoza, and V. L. Brudny, *Phys. Rev. B* **68**, 085318 (2003).

¹⁸S. Roke, W. G. Roeterdink, J. E. G. J. Wijnhoven, A. V. Petukhov, A. W. Kley, and M. Bonn, *Phys. Rev. Lett.* **91**, 258302 (2003).

¹⁹S. Roke, M. Bonn, and A. V. Petukhov, *Phys. Rev. B* **70**, 115106 (2004).

²⁰H. M. Eckenrode and H. L. Dai, *Langmuir* **20**, 9202 (2004).

²¹H. M. Eckenrode, S. H. Jen, J. Han, A. G. Yeh, and H. L. Dai, *J. Phys. Chem. B* **109**, 4646 (2005).

²²J. Nappa, G. Revillod, I. Russier-Antoine, E. Benichou, C. Jonin, and P. F. Brevet, *Phys. Rev. B* **71**, 165407 (2005).

²³R. Jin, J. E. Jureller, H. Y. Kim, and N. F. Scherer, *J. Am. Chem. Soc.* **127**, 12482 (2005).

²⁴S.-H. Jen and H.-L. Dai, *J. Phys. Chem. B* **110**, 23000 (2006).

²⁵J. Nappa, I. Russier-Antoine, E. Benichou, C. Jonin, and P. F. Brevet, *J. Chem. Phys.* **125**, 184712 (2006).

²⁶J. Shan, J. I. Dadap, I. Stioipkin, G. A. Reider, and T. F. Heinz, *Phys. Rev. A* **73**, 023819 (2006).

²⁷L. Schneider, H. J. Schmid, and W. Peukert, *Appl. Phys. B* **87**, 333 (2007).

²⁸I. Russier-Antoine, E. Benichou, G. Bachelier, C. Jonin, and P. F. Brevet, *J. Phys. Chem. C* **111**, 9044 (2007).

²⁹S.-H. Jen, G. Gonella, and H.-L. Dai, *J. Phys. Chem. A* **113**, 4758 (2009).

³⁰S. Roke, *ChemPhysChem* **10**, 1380 (2009).

³¹A. G. F. de Beer, H. B. de Aguiar, J. F. W. Nijsen, and S. Roke, *Phys. Rev. Lett.* **102**, 095502 (2009).

³²S.-H. Jen, H.-L. Dai, and G. Gonella, *J. Phys. Chem. C* **114**, 4302 (2010).

³³S. Viarbitskaya, V. Kapshai, P. van der Meulen, and T. Hansson, *Phys. Rev. A* **81**, 053850 (2010).

³⁴I. Russier-Antoine, J. Duboisset, G. Bachelier, E. Benichou, C. Jonin, N. Del Fatti, F. Vallée, A. Sánchez-Iglesias, I. Pastoriza-Santos, L. M. Liz-Marzan, and P.-F. Brevet, *J. Phys. Chem. Lett.* **1**, 874 (2010).

³⁵J. Butet, G. Bachelier, I. Russier-Antoine, C. Jonin, E. Benichou, and P. F. Brevet, *Phys. Rev. Lett.* **105**, 077401 (2010).

³⁶G. Bachelier, J. Butet, I. Russier-Antoine, C. Jonin, E. Benichou, and P. F. Brevet, *Phys. Rev. B* **82**, 235403 (2010).

³⁷W. Gan, G. Gonella, M. Zhang, and H.-L. Dai, *J. Chem. Phys.* **134**, 041104 (2011).

³⁸J. Martorell, R. Vilaseca, and R. Corbalan, *Phys. Rev. A* **55**, 4520 (1997).

³⁹J. I. Dadap, J. Shan, and T. F. Heinz, *J. Opt. Soc. Am. B* **21**, 1328 (2004).

⁴⁰Y. Pavlyukh and W. Hübner, *Phys. Rev. B* **70**, 245434 (2004).

⁴¹A. G. F. de Beer and S. Roke, *Phys. Rev. B* **79**, 155420 (2009).

⁴²J. I. Dadap, *Phys. Rev. B* **78**, 205322 (2008).

⁴³A. G. F. de Beer and S. Roke, *J. Chem. Phys.* **132**, 234702 (2010).

⁴⁴D. Ostling, P. Stampfli, and K. H. Bennemann, *Z. Phys. D* **28**, 169 (1993).

⁴⁵J. P. Dewitz, W. Hübner, and K. H. Bennemann, *Z. Phys. D* **37**, 75 (1996).

⁴⁶See Appendix of Ref. 39.

- ⁴⁷See Supplemental Material at <http://link.aps.org/supplemental/10.1103/PhysRevB.84.121402> for further details on the NLM theory, experiments, and β elements consistency check.
- ⁴⁸J. D. Jackson, *Classical Electrodynamics*, 2nd ed. (Wiley, New York, 1975).
- ⁴⁹C. F. Bohren and D. R. Huffman, *Absorption and Scattering of Light by Small Particles* (Wiley, New York, 1983).
- ⁵⁰G. M. Hale and M. R. Querry, *Appl. Opt.* **3**, 555 (1973).
- ⁵¹S. N. Kasarova, N. G. Sultanova, C. D. Ivanov, and I. D. Nikolov, *Opt. Mater.* **29**, 1481 (2007).
- ⁵²D. E. Aspnes, *Thin Solid Films* **89**, 249 (1982).
- ⁵³A. Pflüger, *Annalen der Physik* **292**, 412 (1895).
- ⁵⁴H. Du, R.-C. A. Fuh, J. Li, L. A. Corkan, and J. S. Lindsey, *Photochemistry and Photobiology* **68**, 141 (1998).
- ⁵⁵T. Kikteva, D. Star, and G. W. Leach, *J. Phys. Chem. B* **104**, 2860 (2000).
- ⁵⁶T. F. Heinz, H. W. K. Tom, and Y. R. Shen, *Phys. Rev. A* **28**, 1883 (1983).
- ⁵⁷B. Dick, *Chem. Phys.* **96**, 199 (1985).
- ⁵⁸G. J. Simpson and K. L. Rowlen, *J. Am. Chem. Soc.* **121**, 2635 (1999).
- ⁵⁹G. Gonella, H.-L. Dai, H. C. Fry, M. J. Therien, V. Krishnan, A. Tronin, and J. K. Blasie, *J. Am. Chem. Soc.* **132**, 9693 (2010).
- ⁶⁰B. Schürer, S. Wunderlich, C. Sauerbeck, U. Peschel, and W. Peukert, *Phys. Rev. B* **82**, 241404 (2010).